A Self-driving Laboratory Optimizes A Scalable Process For Making Functional Coatings

Connor Rupnow[1] **Benjamin P. MacLeod**[2] **Mehrdad Mokhtari**[2] **Karry Ocean**[2]

Kevan E. Dettelbach[2] **Daniel Lin**[2] **Fraser G. L. Parlane**[2] **Hsi N. Chiu**[2]

Michael B. Rooney[2] **Chris E. B. Waizenegger**[2] **Elija de Hoog**[2] **Curtis P. Berlinguette**[1−4*]

[1]Department of Chemical & Biological Engineering, The University of British Columbia
[2]Department of Chemistry, The University of British Columbia
[3]Stewart Blusson Quantum Matter Institute, The University of British Columbia
[4]Canadian Institute for Advanced Research (CIFAR), MaRS Innovation Centre

[*]cberling@chem.ubc.ca

Abstract

Solution-based coating methods offer low-cost routes to deposit coatings at scale. It is difficult, however, to obtain high quality coatings using these methods due to the complex and dynamic physical and chemical processes involved. Here, we show how a self-driving laboratory can optimize spray-coating, which is relevant to manufacturing a range of clean energy technologies. For this demonstration, we optimized the combustion synthesis of spray-cast conductive palladium films. The closed-loop optimization of this synthesis yielded films with conductivities of >4 MS/m, which compares favorably with the conductivities of 2-6 MS/m reported for thin Pd films obtained by vacuum-based sputtering processes. The champion coating conditions were scaled up to an 8× larger area using the same spray-coating apparatus with no further optimization and no reduction in coating quality or conductivity. This work shows how self-driving laboratories can optimize a scalable process for making functional coatings.

1 Introduction

Large-scale coating methods are essential for manufacturing clean energy technologies such as photovoltaics [1], electrochromics [2] and electrolyzers [3]. Methods for depositing coatings at scale include vacuum-based methods (e.g. sputtering, thermal evaporation) and solution-based methods (e.g. blade coating, inkjet printing, spray-coating). Solution-based coating methods that avoid vacuum and high temperatures offer an opportunity to lower the cost and energy intensity of manufacturing clean energy technologies.

It is often challenging, however, to obtain large, performant and defect-free coatings using solution-based methods [4, 5]. These methods involve a complex interplay between wetting phenomena [6], solvent evaporation [7], solidification processes [8, 9] and, in some cases, chemical reaction kinetics [10]. Moreover, the small-scale processes commonly used to study solution-based coatings in the laboratory (e.g. spin-coating, drop-casting) typically do not translate to large-scale manufacturing. Spray-coating, however, is suitable for coating small substrates for exploratory materials research and larger substrates for manufacturing. Spray-coating is challenging to optimize because it involves numerous experimental variables and objectives [11, 12, 13] (supplementary Fig. S1). Self-driving

36th Conference on Neural Information Processing Systems (NeurIPS 2022).

laboratories present an opportunity to accelerate the development of spray-coating processes suitable for large-scale, low-cost manufacturing of clean energy technologies.

A self-driving laboratory (SDL) consists of an automated experiment controlled by an experiment-planning algorithm. These autonomous laboratories use data from completed experiments to algorithmically plan future experiments. This data-driven approach to experiment planning enables SDLs to optimize material properties and synthesis procedures 10-100× faster than automation alone [14, 15]. While numerous SDLs have implemented lab-scale solution-based coating methods [16, 15, 17, 18, 19], a self-driving laboratory for optimizing large-scale solution-based coating processes has not yet been reported. Here, we use a self-driving laboratory to optimize a spray-coating deposition process (Fig. 1).

To autonomously optimize spray-coating processes, we leveraged flexible automation to upgrade our existing SDL [16, 15], "Ada", with a purpose-built ultrasonic spray-coater (see Figs. 1a-d, supplementary methods). We designed this spray-coater to enable rapid, automated spray-coating experiments. Ada iteratively optimizes the spray-coating process and precursor ink composition under the control of a Bayesian optimization algorithm [20] (see inset to Fig. 1a and supplementary methods). Ada uses a parallelized workflow (Fig. 1e) to perform up to 100 spray-coating experiments per day without human intervention. Here, we demonstrate the power of this platform by using it to optimize the conductivity of spray-coated palladium films (Fig. 1f) by manipulating seven variables simultaneously.

2 Results & Discussion

Conductive palladium coatings have applications in fuel cells [21], CO2 utilization [22], and electrochemical hydrogenation [23, 24]. and can be deposited from solution using a technique known as spray-combustion synthesis [10, 25, 26, 15]. In our previous study [15], we observed that combustion-synthesized Pd films made by drop-casting exhibit a trend of increasing film conductivity with annealing temperature up to 280 °C. Here, we found that spray-coating the same precursors failed to deposit continuous films at 250 °C (Fig. S2), showcasing how the translation of a laboratory coating technique (drop-casting) to a more scalable manufacturing technique (spray-coating) can create unanticipated difficulties. This finding motivated us to optimize the precursor ink and spray-coating process variables simultaneously.

We configured Ada to autonomously maximize the Pd film conductivity by manipulating seven experimental variables that control the spray-coating process (Fig. 2, Table S1). Each manipulated variable was chosen according to a hypothesis. Hotplate temperature was varied because higher synthesis temperatures are known to improve charge transport in combustion synthesized films [10, 15]. Precursor concentration was varied because it influences overall film thickness, which can influence conductivity through percolation and boundary scattering effects [27, 28]. The number of spray-coating passes was varied because it influences the thickness of the reacting precursor layer, which is known to control film porosity in combustion-synthesized films and may thus impact conductivity [10]. Spray nozzle height, precursor ink flowrate, and air flowrate were varied because these variables are known to impact the roughness of spray-coated films [11] and roughness tends to decrease film conductivity [29]. DMSO content was varied because our initial observations (see Fig. S2) and literature data both showed that adding a co-solvent with a high boiling point has the ability to increase the temperature at which coatings can be deposited by spraying [30]. The ranges of values over which each variable was manipulated are shown as the minimum and maximum y-value of each axis in Fig. 2b.

Ada optimized the Pd film conductivity in a closed loop by autonomously performing 91 cycles of precursor preparation, spray-coating, film characterization and algorithmic experiment planning (see Fig. 1a inset). In each cycle, a unique experimental condition was tested in duplicate (except for rare instances where duplicates were missed due to system failures). Each experimental cycle involved 7 steps, all of which were performed autonomously by Ada (see supplementary methods - autonomous workflow step 1-7). Ada began each experimental cycle by requesting an experimental condition to test from an experimental planning algorithm. To initialize this algorithm, the first 15 experimental conditions were chosen at random from a uniform random distribution over the input space (see supplementary methods - step 1). The precursor mixing station then prepared 0.38 mL of spray-coating precursor ink in a 2-mL vial (see supplementary methods - step 2). The

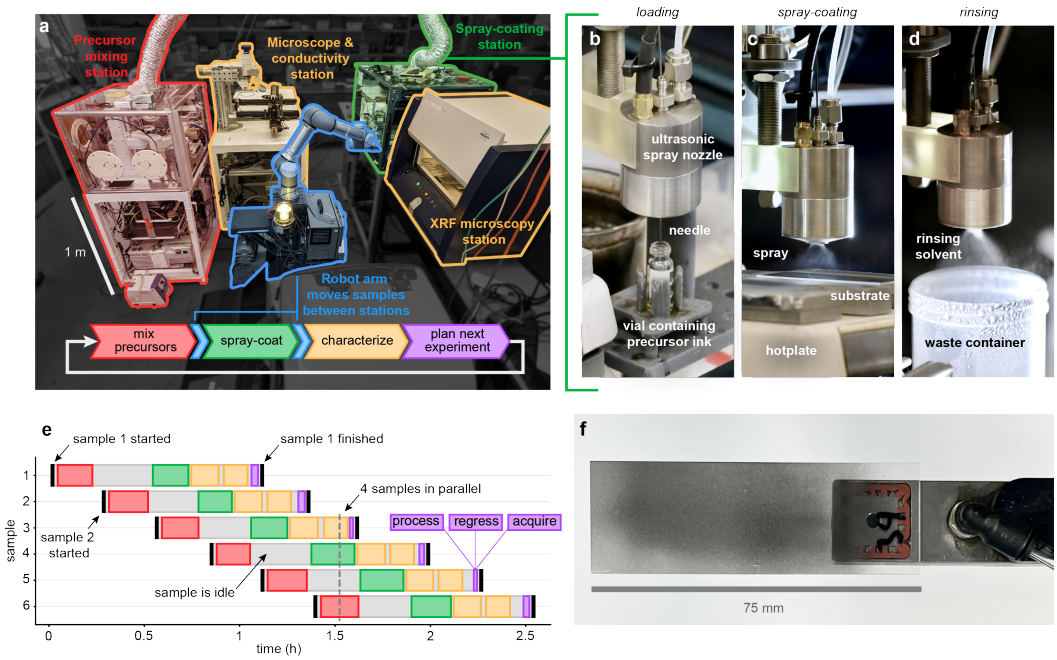

Figure 1: Ada - A self-driving laboratory designed to optimize scalable spray-coating processes. **(a)** The self-driving laboratory consists of two synthesis and two characterization stations linked together by a central 6-axis robotic arm. This robotic arm transports spray-coating precursor inks (in 2-mL vials, see panel b) and thin-film samples (on 75 mm × 25 mm glass substrates, see panel f) between stations as required to execute the parallelized closed-loop optimization workflow (shown in simplified serial form in panel a inset and in full detail in panel e). **(b-d)** The spray-coating station has been custom designed to load precursor inks through a retractable needle at the front of the nozzle (panel b), Front-loading minimizes the volume of precursor ink required to prime the nozzle and enables small volumes (< 1mL) of precursor ink to be sprayed. The loaded precursor ink is sprayed on to a heated substrate to form a coating (panel c). When spraying is complete, residual precursor ink is automatically rinsed out of the nozzle (panel d). **(e)** The parallelized workflow for the optimization campaign. Ada's "station" architecture enables Ada to work on up to four samples in parallel. This parallel workflow enables up to one hundred spray-coating experiments per day. For clarity, the durations of the very short (<1 min.) experiment planning steps are not shown to scale. The experiment planning process consists of three steps: data processing, Gaussian process regression, and acquisition of new experimental conditions. **(f)** The Pd film sample (left) is moved between stations by the 6-axis robotic arm using a vacuum handler (right).

precursor ink vial and a clean 25 mm × 75 mm glass substrate were then transported from the precursor mixing station to the spray-coating station by the central robotic arm. The precursor ink was then sprayed onto a pre-heated glass substrate to form an approximately 10 to 100-nm thick Pd coating (see supplementary methods - step 3). With the sample synthesis complete, the robotic arm then picked up the completed sample and passed it to the other stations for fully automated characterization. The Pd coating thickness was measured by X-ray fluorescence microscopy (XRF) (see supplementary methods - step 4). The coating conductance was measured via four-point probe (see supplementary methods - step 5). Each film was also imaged using an optical microscope (see supplementary methods - step 5). The Pd coating sample was then returned to a storage rack. The coating conductivity was calculated by combining conductance and thickness measurements (see supplementary methods - step 6). To complete each cycle, the experimental data generated (i.e. the experimental conditions tested and the resulting coating conductivity) was processed and then passed to a single objective Bayesian optimizer. The optimizer then selected the next experimental condition to test using all the data available from previously completed samples (see supplementary methods - step 7).

To maximize experimental throughput, Ada was configured so that all hardware stations operated on different samples in parallel. This configuration enabled the system to work on up to four samples at any one time (see Fig. 1e). This parallelization scheme increased experimental throughput by 300% but required the experiment planning algorithm to plan new experiments while the last three requested samples were not yet complete. In this situation, a conventional Bayesian optimizer designed for serial experiments would repeatedly request the same experimental conditions, a potentially undesirable behaviour. To avoid excessively replicating the same experimental condition, we configured the optimizer with an acquisition function that alternated between four modes. The first three modes used the upper confidence bound acquisition function with $\beta = 0.25$, 25, and 400, respectively. The fourth mode selected a space-filling point (i.e. a point as far as possible from any previously tested point in the input space, see supplementary methods - space-filling point) based on a suggestion by Schmidt et al. that sampling space-filling points may improves Bayesian optimizer performance on rough response surfaces [31]. This 4-mode acquisition function balances exploitation and exploration, avoids suggesting replicate samples and ensures robust explorative behaviour by choosing space filling points in a way that does not depend on the quality of the surrogate model. Further details of the optimizer configuration are provided in the supplementary methods (see supplementary methods - autonomous workflow step 7).

The results of the optimization are shown in Fig. 2. The experimental condition yielding the highest mean conductivity across duplicates was identified after 63 cycles of experimentation (Fig. 2a). This champion experiment with a conductivity of 4.08 MS/m doubles the best previously reported value of 2.0 MS/m for Pd films deposited by spray-combustion [15] and is comparable to the conductivities of sputtered films which range from 2 to 6 MS/m [28, 32]. The relative conductivity difference between the duplicate samples created using the champion experimental conditions was less than 1% (see SI for a discussion of the experimental variability and possible sources thereof).

Ada tested a large number of diverse experimental conditions over the course of the optimization campaign (Fig. 2b). This rich data provides insights about the Pd spray-combustion process beyond the simple identification of conditions that maximize the film conductivity. Most strikingly, the data reveal that the film conductivity was strongly correlated with thickness (see Fig. S3). We attribute this observation to the gradual percolation of conductive Pd islands as the film thickness increases, as has been observed, for example with nanogranular gold films [27] (we note that our Pd films show nano-granularity in SEM images, see Fig. S4). Given the strong observed correlation between Pd film conductivity and thickness, we were able to identify explanations for the optimal spray-coating conditions that are supported by data from the optimization campaign, follow-up experiments and the literature.

Ada identified a high precursor concentration (20 mg/mL) as optimal (see Fig. 2b, precursor concentration). High precursor concentration increases film thickness (and thus conductivity) by simply adding more Pd to the film (see Fig. S5).

Ada found that the lowest allowed nozzle height (10 mm) was optimal (see Fig. 2b, nozzle height). Low nozzle height increases film thickness (and thus conductivity) by reducing overspray and thus depositing a larger fraction of the precursor onto the substrate (see Fig. S5).

The optimal values for the remaining input parameters appear to arise due to a complex interplay between the film thickness, the precursor composition, the spray-coating conditions, the local substrate temperature and the Leidenfrost effect. The Leidenfrost effect occurs when a droplet of a liquid impinging on a hot surface becomes suspended on a cushion of its own vapour. This effect is known to slow or prevent film deposition of spray-coated materials at high temperatures by repelling precursor droplets from the heated substrate [30]. Fluid phenomena such as the Leidenfrost effect create complex relationships between coating conditions and outcomes. This complexity can make it difficult to transfer knowledge from one coating method to another (e.g. from drop-casting to spray-coating as found here).

Ada identified an intermediate temperature (258.6 °C) as optimal (see Fig. 2b, hotplate temperature). This optimum appears to avoid the detrimental Leidenfrost effect that would occur at higher temperatures while providing sufficient thermal energy to drive the combustion of the precursor [15, 26].

Ada found that adding large amounts of DMSO (30% v/v) into the precursor ink maximized the conductivity (see Fig. 2b, DMSO content). The beneficial effect of DMSO appears to arise from the

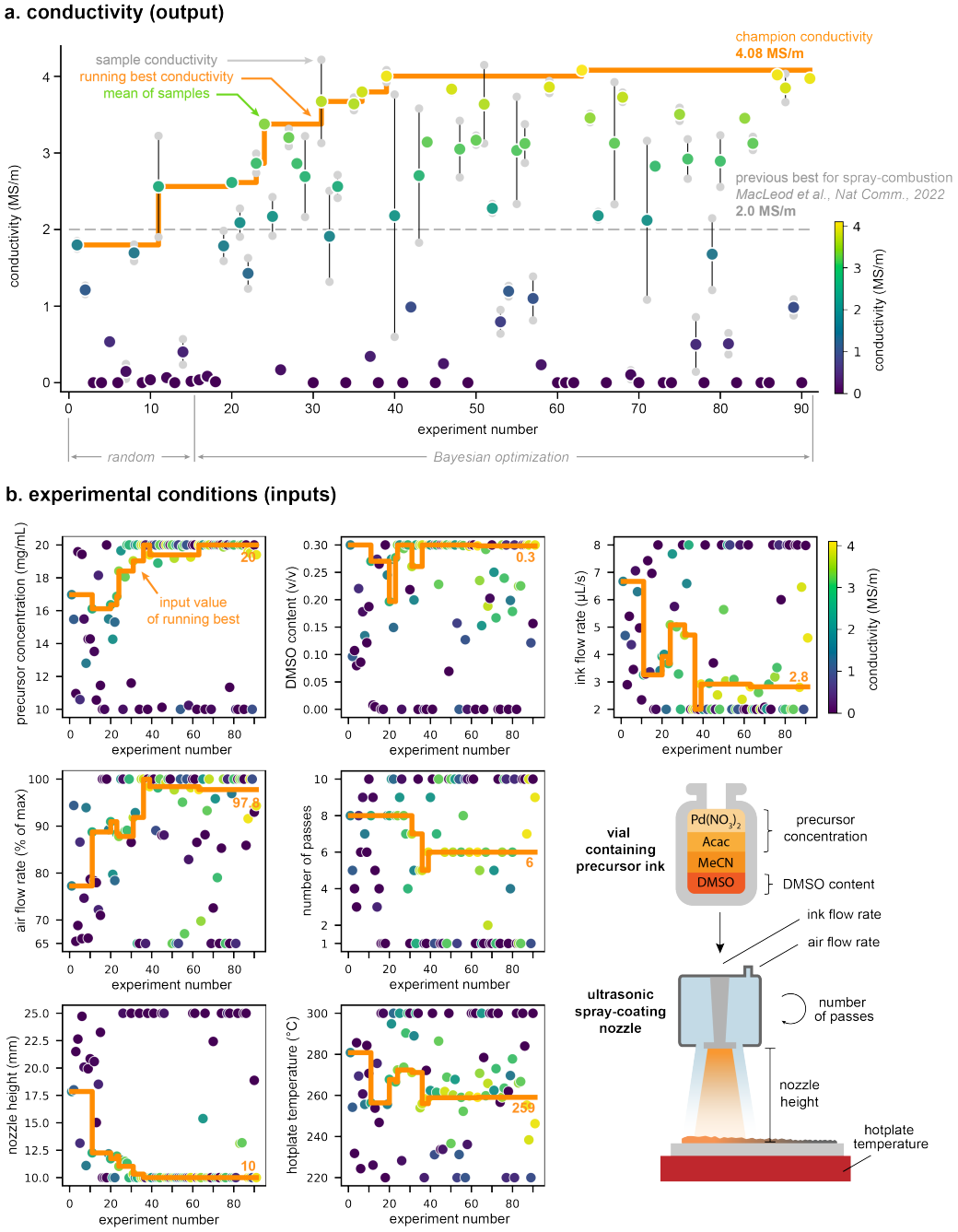

Figure 2: Autonomous optimization of the conductivity of a spray-coated palladium film. **(a)** Bayesian optimization was performed over 91 experiments. Each experiment was performed in duplicate and a maximum mean conductivity of 4.08 MS/m was achieved, more than double the previous best for spray-combustion. The orange line represents the running best conductivity over time. **(b)** Seven input variables were manipulated: two ink composition variables (DMSO content and solute concentration) and five spray-coating variables (ink flowrate, air flowrate, number of passes, height, and hotplate temperature). The experimental conditions requested for each experiment are shown in each plot. The orange line represents the input values associated with the running best conductivity. The input value yielding the champion recipe is shown at the end of each orange line.

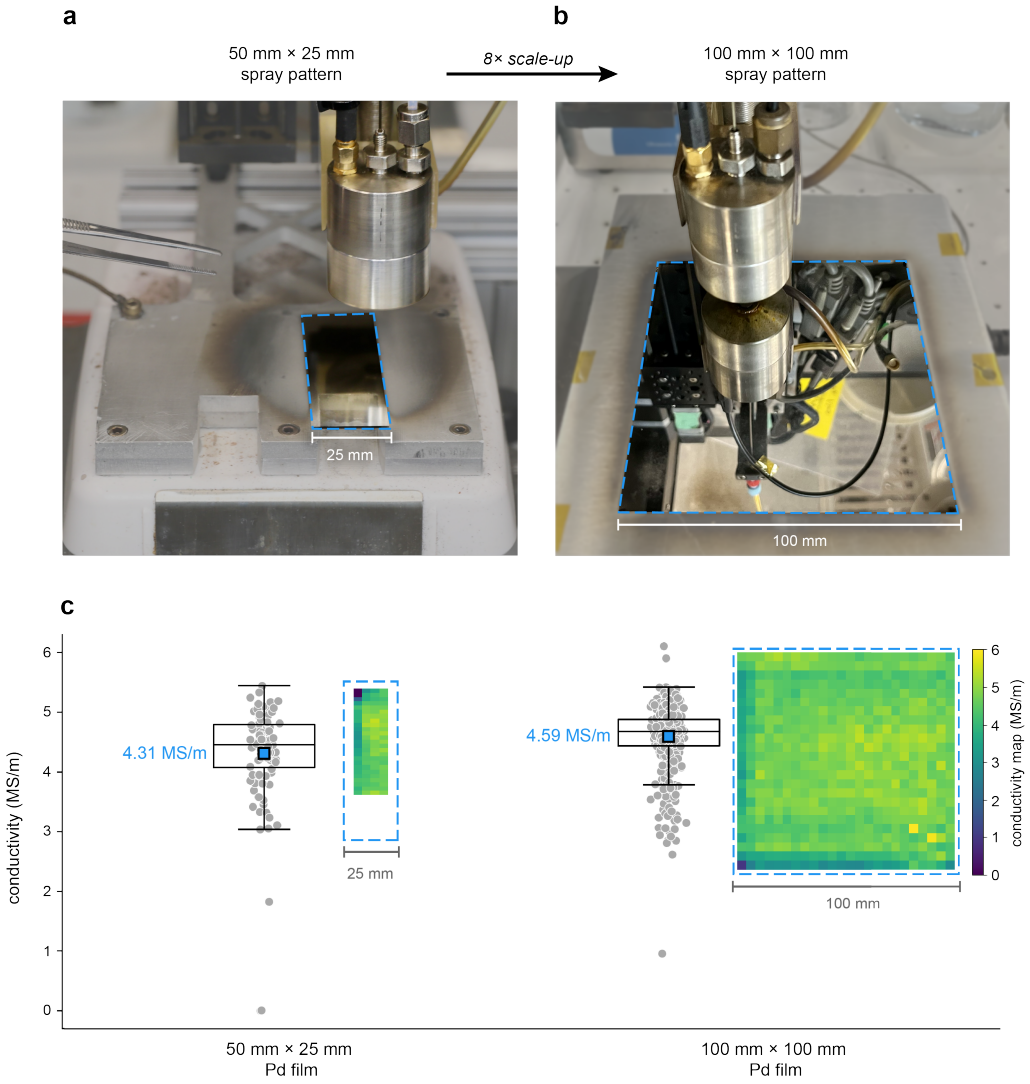

Figure 3: The identified champion coating conditions were scaled-up to an 8× larger area with no further optimization and with no loss in coating conductivity.
The champion conditions identified by the optimization campaign were successfully scaled-up from **(a)** 50 mm × 25 mm to **(b)** 100 mm × 100 mm, to create a coating of 8× larger area with no modifications other than the requisite increase in the size of the nozzle pattern and ink volume (see supplementary Fig. S10). **(c)** Conductivity measurements performed on both samples showed comparable conductivities for both the small-scale and the large-scale samples (see supplementary methods - scale-up experiment). The larger film was slightly more conductive and uniform than the smaller film, exhibiting a conductivity of 4.59 ± 0.49 MS/m and 4.31 ± 0.86 MS/m, respectively.

suppression of the Leidenfrost effect. This is because DMSO (T_{vap} = 189 °C) is a higher boiling solvent than the other solvent used in our precursor inks (acetonitrile, T_{vap} = 82 °C) (Fig. S6). To support this conclusion, we used Ada to perform a series of follow-up experiments that show that inks containing DMSO result in thicker Pd films at higher temperatures (Fig. S7).

Ada found that a high flow rate of air from the nozzle (control valve opened to 97.8% of the maximum) was optimal (see Fig. 2b, air flow rate). We attribute this to suppression of the Leidenfrost effect caused by transient cooling of the substrate by this impinging airflow. Transient cooling enables the precursor to efficiently coat the substrate by avoiding the Leidenfrost effect, while subsequent reheating of the substrate promotes the complete transformation of the precursor into metallic Pd. Thermography and thermocouple data show that the nozzle causes rapid transient cooling and reheating of the substrates in our system, with temperature swings as large as 30 °C (see Fig. S8). Stronger transient cooling of the substrate may also be an additional benefit of low nozzle height.

Ada found that low flow rate of ink from the nozzle (2.8 uL/s) was optimal (see Fig. 2b, ink flow rate). Since the ink volume sprayed was fixed, lower ink flow rates lead to slower nozzle speeds. This caused the nozzle to remain over the substrate for longer, providing more time for the air from the nozzle to locally cool the surface and further suppress the Leidenfrost effect (see Figs. S8, S9).

The number of spray-coating passes appeared to be the least important manipulated variable; high conductivity films were obtained across all settings for this variable (see Fig. 2b, number of passes).

The optimal experimental conditions identified by Ada balance the complex, inter-related effects described above to form highly conductive palladium films.

Following the optimization campaign, the conditions yielding the champion Pd film were scaled-up to a larger area with no further optimization and no reduction in coating quality (Fig. 3). Specifically, we used the same champion conditions and the same spray-coater used for the optimization campaign to deposit a Pd film on a 100 mm × 100 mm glass substrate (see supplementary methods - scale-up experiment). The scaled-up spray-coating process yielded a highly reflective large-area Pd film that had a higher and more uniform conductivity (4.59 ± 0.49 MS/m) than the small-scale samples autonomously optimized by Ada (4.31 ± 0.86 MS/m). We expect this spray-coating process to scale to even larger areas so long as the process conditions (e.g. substrate temperature) can be held sufficiently uniform across the substrate. Our success in scaling-up the champion recipe with no further optimization highlights the value of directly optimizing a scalable coating process such as spray-coating using a self-driving laboratory.

3 Limitations and potential societal impacts

The resources and expertise currently required to deploy and operate self-driving laboratories currently limit both their potential positive and negative societal impacts. We believe a valuable direction for future work is to develop self-driving laboratories that require fewer resources and less expertise to deploy and operate. A deeper consideration of the potential negative societal impacts of these systems will become necessary as self-driving laboratories become more widely available.

4 Conclusion

We used a self-driving laboratory to optimize a complex spray-combustion process for depositing conductive palladium coatings. This optimization campaign discovered conditions for preparing highly conductive Pd coatings (>4 MS/m) by spray-coating. The optimal coating conditions identified by the self-driving laboratory were readily scaled-up from 1250 mm^2 to a 10000 mm^2 film without compromising the conductivity. The rich data generated by the self-driving laboratory also yielded insights into the complex processes at play during the spray-combustion synthesis of Pd coatings. This work shows how self-driving laboratories can be used to address the challenges associated with scaling up solution-based coating methods.

Data availability

The raw and processed data generated by the self-driving laboratory in this study is available at `https://github.com/berlinguette/ada`. All other data related to this paper is available from

the corresponding author upon request. All code used in this study was based on open-source Python packages listed in the supplementary information.

Acknowledgements

The authors are grateful to Natural Resources Canada's Energy Innovation Program (EIP2-MAT-001), the Canadian Natural Science and Engineering Research Council (RGPIN-2018-06748), Canadian Foundation for Innovation (229288), Canadian Institute for Advanced Research (BSE-BERL-162173), and Canada Research Chairs for financial support. The authors are also thankful to Oliver Horner and Abhishek Soni for their assistance.

References

[1] Jin Yan, Tom J Savenije, Luana Mazzarella, and Olindo Isabella. Progress and challenges on scaling up of perovskite solar cell technology. *Sustainable Energy Fuels*, 6(2):243–266, January 2022.

[2] Guofa Cai, Jiangxin Wang, and Pooi See Lee. Next-Generation multifunctional electrochromic devices. *Acc. Chem. Res.*, 49(8):1469–1476, August 2016.

[3] Tingting Zheng, Kun Jiang, Na Ta, Yongfeng Hu, Jie Zeng, Jingyue Liu, and Haotian Wang. Large-Scale and highly selective CO2 electrocatalytic reduction on nickel Single-Atom catalyst. *Joule*, 3(1):265–278, January 2019.

[4] David Mitzi. *Solution Processing of Inorganic Materials*. John Wiley & Sons, December 2008.

[5] Nina Taherimakhsousi, Benjamin P MacLeod, Fraser G L Parlane, Thomas D Morrissey, Edward P Booker, Kevan E Dettelbach, and Curtis P Berlinguette. Quantifying defects in thin films using machine vision. *npj Computational Materials*, 6(1):1–6, July 2020.

[6] J Z Wang, Z H Zheng, H W Li, W T S Huck, and H Sirringhaus. Dewetting of conducting polymer inkjet droplets on patterned surfaces. *Nat. Mater.*, 3(3):171–176, March 2004.

[7] B T Chen. Investigation of the solvent-evaporation effect on spin coating of thin films. *Polym. Eng. Sci.*, 23(7):399–403, May 1983.

[8] Iñigo Bretos, Stefano Diodati, Ricardo Jimenez, Francesca Tajoli, Jesus Ricote, Giulia Bragaggia, Marina Franca, Maria Lourdes Calzada, and Silvia Gross. Low-temperature solution crystallization of nanostructured oxides and thin films. *Chemistry*, March 2020.

[9] Ajay A Virkar, Stefan Mannsfeld, Zhenan Bao, and Natalie Stingelin. Organic semiconductor growth and morphology considerations for organic thin-film transistors. *Adv. Mater.*, 22(34):3857–3875, September 2010.

[10] Myung-Gil Kim, Mercouri G Kanatzidis, Antonio Facchetti, and Tobin J Marks. Low-temperature fabrication of high-performance metal oxide thin-film electronics via combustion processing. *Nat. Mater.*, 10(5):382–388, May 2011.

[11] Sanjukta Bose, Stephan S Keller, Tommy S Alstrøm, Anja Boisen, and Kristoffer Almdal. Process optimization of ultrasonic spray coating of polymer films. *Langmuir*, 29(23):6911–6919, June 2013.

[12] Zhe Liu, Nicholas Rolston, Austin C Flick, Thomas W Colburn, Zekun Ren, Reinhold H Dauskardt, and Tonio Buonassisi. Machine learning with knowledge constraints for process optimization of open-air perovskite solar cell manufacturing. *Joule*, 6(4):834–849, April 2022.

[13] A Schneider, N Traut, and M Hamburger. Analysis and optimization of relevant parameters of blade coating and gravure printing processes for the fabrication of highly efficient organic solar cells. *Sol. Energy Mater. Sol. Cells*, 126:149–154, July 2014.

[14] Sebastian Ament, Maximilian Amsler, Duncan R Sutherland, Ming-Chiang Chang, Dan Guevarra, Aine B Connolly, John M Gregoire, Michael O Thompson, Carla P Gomes, and R Bruce van Dover. Autonomous materials synthesis via hierarchical active learning of nonequilibrium phase diagrams. *Science Advances*, 7(51):eabg4930, 2021.

[15] Benjamin P MacLeod, Fraser G L Parlane, Connor C Rupnow, Kevan E Dettelbach, Michael S Elliott, Thomas D Morrissey, Ted H Haley, Oleksii Proskurin, Michael B Rooney, Nina Taherimakhsousi, David J Dvorak, Hsi N Chiu, Christopher E B Waizenegger, Karry Ocean, Mehrdad Mokhtari, and Curtis P Berlinguette. A self-driving laboratory advances the pareto front for material properties. *Nat. Commun.*, 13(1):1–10, February 2022.

[16] B P MacLeod, F G L Parlane, T D Morrissey, F Häse, L M Roch, K E Dettelbach, R Moreira, L P E Yunker, M B Rooney, J R Deeth, V Lai, G J Ng, H Situ, R H Zhang, M S Elliott, T H Haley, D J Dvorak, A Aspuru-Guzik, J E Hein, and C P Berlinguette. Self-driving laboratory for accelerated discovery of thin-film materials. *Sci Adv*, 6(20):eaaz8867, May 2020.

[17] Stefan Langner, Florian Häse, José Darío Perea, Tobias Stubhan, Jens Hauch, Loïc M Roch, Thomas Heumueller, Alán Aspuru-Guzik, and Christoph J Brabec. Beyond ternary OPV: High-Throughput experimentation and Self-Driving laboratories optimize multicomponent systems. *Adv. Mater.*, 32(14):e1907801, April 2020.

[18] Daniil Bash, Yongqiang Cai, Vijila Chellappan, Swee Liang Wong, Xu Yang, Pawan Kumar, Jin Da Tan, Anas Abutaha, Jayce J W Cheng, Yee-Fun Lim, Siyu Isaac Parker Tian, Zekun Ren, Flore Mekki-Berrada, Wai Kuan Wong, Jiaxun Xie, Jatin Kumar, Saif A Khan, Qianxiao Li, Tonio Buonassisi, and Kedar Hippalgaonkar. Multi-fidelity high-throughput optimization of electrical conductivity in P3HT-CNT composites. *Adv. Funct. Mater.*, 31(36):2102606, September 2021.

[19] Zhi Li, Mansoor Ani Najeeb, Liana Alves, Alyssa Z Sherman, Venkateswaran Shekar, Peter Cruz Parrilla, Ian M Pendleton, Wesley Wang, Philip W Nega, Matthias Zeller, Joshua Schrier, Alexander J Norquist, and Emory M Chan. Robot-Accelerated perovskite investigation and discovery. *Chem. Mater.*, 32(13):5650–5663, July 2020.

[20] BoTorch · bayesian optimization in PyTorch. `https://botorch.org/tutorials/multi_objective_bo`. Accessed: 2022-9-24.

[21] Jong Seon Park, Hyung Jong Choi, Gwon Deok Han, Junmo Koo, Eun Heui Kang, Dong Hwan Kim, Kiho Bae, and Joon Hyung Shim. High–performance protonic ceramic fuel cells with a PrBa0.5Sr0.5Co1.5Fe0.5O5+δ cathode with palladium–rich interface coating. *J. Power Sources*, 482:229043, January 2021.

[22] Dunfeng Gao, Hu Zhou, Fan Cai, Jianguo Wang, Guoxiong Wang, and Xinhe Bao. Pd-Containing nanostructures for electrochemical CO2 reduction reaction. *ACS Catal.*, 8(2):1510–1519, February 2018.

[23] Rebecca S Sherbo, Aiko Kurimoto, Christopher M Brown, and Curtis P Berlinguette. Efficient electrocatalytic hydrogenation with a palladium membrane reactor. *J. Am. Chem. Soc.*, 141(19):7815–7821, May 2019.

[24] Roxanna S Delima, Rebecca S Sherbo, David J Dvorak, Aiko Kurimoto, and Curtis P Berlinguette. Supported palladium membrane reactor architecture for electrocatalytic hydrogenation. *J. Mater. Chem. A Mater. Energy Sustain.*, 7(46):26586–26595, November 2019.

[25] Xinge Yu, Jeremy Smith, Nanjia Zhou, Li Zeng, Peijun Guo, Yu Xia, Ana Alvarez, Stefano Aghion, Hui Lin, Junsheng Yu, Robert P H Chang, Michael J Bedzyk, Rafael Ferragut, Tobin J Marks, and Antonio Facchetti. Spray-combustion synthesis: efficient solution route to high-performance oxide transistors. *Proc. Natl. Acad. Sci. U. S. A.*, 112(11):3217–3222, March 2015.

[26] Albert A Voskanyan, Chi-Ying Vanessa Li, and Kwong-Yu Chan. Catalytic palladium film deposited by scalable Low-Temperature aqueous combustion. *ACS Appl. Mater. Interfaces*, 9(38):33298–33307, September 2017.

[27] M Mirigliano, F Borghi, A Podestà, A Antidormi, L Colombo, and P Milani. Non-ohmic behavior and resistive switching of au cluster-assembled films beyond the percolation threshold. *Nanoscale Advances*, 1(8):3119–3130, 2019.

[28] Y S Shi. Electrical resistivity of RF sputtered pd films. *Phys. Lett. A*, 319(5):555–559, December 2003.

[29] E Z Luo, S Heun, M Kennedy, J Wollschläger, and M Henzler. Surface roughness and conductivity of thin ag films. *Phys. Rev. B Condens. Matter*, 49(7):4858–4865, February 1994.

[30] Ulrich P Muecke, Gary L Messing, and Ludwig J Gauckler. The leidenfrost effect during spray pyrolysis of nickel oxide-gadolinia doped ceria composite thin films. *Thin Solid Films*, 517(5):1515–1521, January 2009.

[31] Mohamed Osama, Bobak Shahriari, and Mark Schmidt. Do we need "harmless" bayesian optimization and "First-Order" bayesian optimization? `https://bayesopt.github.io/papers/2016/Ahmed.pdf`, 2016. Accessed: 2022-10-27.

[32] R Anton, K Häupl, P Rudolf, and P Wißmann. Electrical and structural properties of thin palladium films. *Zeitschrift für Naturforschung A*, 41(4):665–670, April 1986.